ELSEVIER

Contents lists available at ScienceDirect

# Journal of Colloid and Interface Science

www.elsevier.com/locate/jcis



## **Short Communication**

# Thermodynamic cycle analysis for capacitive deionization

# P.M. Biesheuvel

Department of Environmental Technology, Wageningen University, Bomenweg 2, 6703 HD Wageningen, The Netherlands Wetsus, Centre of Excellence for Sustainable Water Technology, Agora 1, 8900 CC Leeuwarden, The Netherlands

#### ARTICLE INFO

### Article history: Received 26 September 2008 Accepted 1 December 2008 Available online 22 January 2009

Keywords: Capacitive deionization Desalination Diffuse double layer theory Thermodynamic cycle analysis

#### ABSTRACT

Capacitive deionization (CDI) is an ion removal technology based on temporarily storing ions in the polarization layers of two oppositely positioned electrodes. Here we present a thermodynamic model for the minimum work required for ion separation in the fully reversible case by describing the ionic solution as an ideal gas of pointlike particles. The work input is fully utilized to decrease the entropy of the outflowing streams compared to that of the inflow. Based on the Gouy–Chapman–Stern (GCS) model for planar diffuse polarization layers—with and without including additional ion volume constraints in the diffuse part of the double layer—we analyze the electric work input during charging and the work output during discharging, for a reversible charging—discharging cycle. We present a graphical thermodynamic cycle analysis for the reversible net work input during one full cycle of batchwise operation of CDI based on the charge—voltage relations for different ionic strengths. For the GCS model, an analytical solution is derived for the charge efficiency  $\Lambda$ , which is the number of salt molecules removed per electron transferred from one electrode to the other. Only in the high voltage limit and for an infinite Stern layer capacity does  $\Lambda$  approach unity.

© 2008 Elsevier Inc. All rights reserved.

#### 1. Introduction

When two electrodes are placed opposite to one another, and a voltage difference is applied, diffuse polarization layers develop on both electrodes. Taken together, the two polarization layers contain an excess of salt ions over the ion concentration in bulk solution, and thus effectively part of the ions in the solution phase is removed. The removal of ions according to this principle from an (aqueous) stream flowing along the electrodes is called capacitive deionization (CDI) or electrosorption desalination [1-4]. The topic is closely related to research in the field of electric double layer (super-)capacitors [5-26]. Important in CDI is the creation of a large surface area for ion storage, and therefore materials such as porous activated carbon are often used (with internal surface areas of the order of  $10^3$  m<sup>2</sup>/g) [5]. Ion adsorption can be continued until the equilibrium structure of the polarization layer is formed and the final capacity for ion storage is reached. In the discharge step, the applied voltage is reduced (gradually, or by short-circuiting the electronic path) resulting in a discharge of the ion storage capacity, and a product stream concentrated in ions, after which a new cycle can begin.

In this manuscript we discuss several thermodynamic and electrostatic aspects of CDI. First we present a macroscopic thermodynamic analysis of CDI to calculate the minimum work required

to separate an ionic solution in a more dilute and a more concentrated stream. In this analysis we describe the ionic solution as a perfect ideal gas of pointlike charges without volume, which is also the common model underlying the Poisson-Boltzmann equation and the Gouy-Chapman (GC) model. Subsequently we analyze several microscopic models for charging of the polarization layers to discuss the work in- and output during the ion removal step (charging of the electrodes) and during the ion release step (discharge of the electrodes). Here we will use the GC model, the Gouy-Chapman-Stern (GCS) model, as well as a modified GCS model which additionally includes ion volume effects in the diffuse part of the double layer, using an off-lattice algorithm from liquid-state theory (the Carnahan-Starling equation of state) which is very exact in describing volume exclusion effects in hard-sphere mixtures [27]. Only by using this final modification are unrealistically high ion concentrations at the Stern plane avoided. In all cases we take the electrode as perfectly conducting with the free electrons directly located at the metal-solution interface. Thus we will neglect the potential difference over the thin layer in the metal (and slightly on the outside of it) where the free electrons are located (the Thomas-Fermi layer), and do not consider the electron overspill into the aqueous solution [5]. We will assume that the two electrodes are perfectly non-Faradaic, i.e., no current is assumed to flow via electrochemical reactions from the electrodes into solution or vice versa. Also, we neglect the possibility of direct chemical ion adsorption or desorption on the electrode surface; i.e., the electrode is assumed to be uncharged when in contact with water and when the electron charge is zero. An ionic charge only develops when an electron charge is applied, and is due to the diffuse charge from the excess of counterions and the depletion of co-ions. This diffuse layer charge is exactly compensated for by the free electron charge residing at the electrode-solution interface. A planar structure of the polarization layer is assumed, and double layer overlap is neglected, which however should be included in a more detailed model [5,23]. These double layer models will be used in a thermodynamic cycle analysis which shows the energy requirements (and losses) of the individual charging and discharging steps in CDI.

An important element in the cycle analysis is the charge efficiency,  $\Lambda$ , which describes how many salt ions are removed for each electron transferred from one electrode to the other, i.e., the ratio of moles of ions removed from solution over the electrode charge (divided by Faraday's number). Because the electron surface charge is compensated in the diffuse layer by both an adsorption of counterions as well as a depletion of co-ions [3,6], the charge efficiency  $\Lambda$  will always be below unity. At very low applied voltages over the diffuse part of the double layer (Debye–Hückel limit),  $\Lambda$  approaches zero because in that limit the diffuse charge is equally due to counterion adsorption as to co-ion expulsion, and thus no ions will be effectively removed from solution on applying a cell voltage. Due to this effect high voltages are preferred for operation in CDI, not just to obtain a high surface charge but also to obtain a high charge efficiency  $\Lambda$ .

# 2. Overall thermodynamic model for capacitive deionization

In this section we describe the thermodynamics of separating an ionic solution into two different solutions, one enriched in ions, the other depleted partially from the ions (see Fig. 1) somewhat similar to a treatment in Ref. [9]. The volume is conserved (the solvent is incompressible) as well as the total number of ions.

Interestingly, this problem is thermodynamically completely analogous to the situation of having a closed (say, cylindrical) vessel filled with an ideal gas. From one end of the cylinder a piston is pushed through up to a certain position, thereby compressing the gas by a certain factor. The volume that is moved through and is "left behind" does not become completely devoid of gas molecules because the piston is assumed to be somewhat "leaky" during its movement. This volume corresponds to the dilute (ion depleted) product stream formed in CDI, while the compartment with compressed gas corresponds to the product stream which is concentrated in ions. When the piston moves very slowly and without friction from its starting point to the final location, the process is reversible and the required work input is the absolute minimum, corresponding to the entropy decrease of the system. Fig. 1 shows that for the fully reversible case, without heat production due to friction, the net work input  $W_{in} - W_{out}$  is exactly balanced by the entropy decrease of the outflowing streams relative to the entropy of the inflowing stream.

We will quantitatively analyze the thermodynamics of ion removal based on an inflowing stream with volume  $V_0$  (note that volume V can be considered as a volumetric flow rate as well), containing one type of monovalent salt which is fully dissociated into cations and anions. The concentration of ions c is the ionic strength (half the total number density of ions). The aim is to separate this solution into a more concentrated solution "c", and a more dilute one, "d" (see Fig. 1). Because we will neglect all interactions between the ions and thus describe the ion solution as an ideal gas of point charges without volume, the only contribution to the free energy is due to ideal entropy. By definition the entropy of the two product solutions is lower than before (the two product solutions will spontaneously mix when allowed to) and thus a certain amount of work needs to be expended in any process to

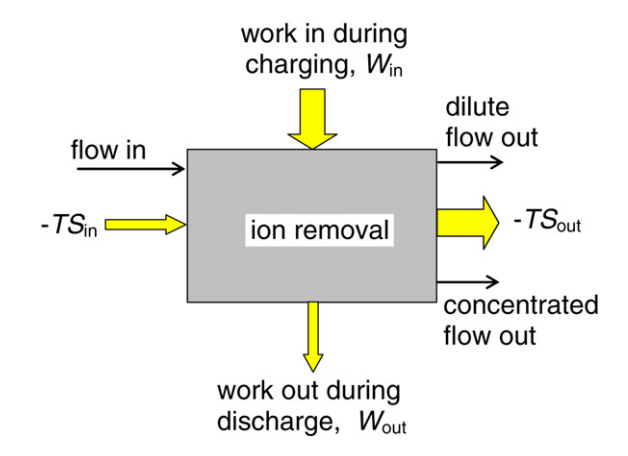


**Fig. 1.** Schematic representation of thermodynamics in an ideal ion removal technology. The free energy of the product streams (right-hand side) is larger than that of the inflowing stream (left), due to a decrease of the entropy TS. This difference is exactly equal to the total reversible work input  $W_{\rm in} - W_{\rm out}$ .

separate an ionic solution into a more dilute and a more concentrated fraction.

An overall ion number balance applies, which is given by  $V_0 \cdot c_0 = V_c \cdot c_c + V_d \cdot c_d$ , as well as a solution volume balance,  $V_0 = V_c + V_d$ . The minimum work that must be exerted on the system under ideal reversible conditions is defined as W which is equal to the difference of work input  $W_{\rm in}$  and work output  $W_{\rm out}$  (see Fig. 1); thus  $W = W_{\rm in} - W_{\rm out}$ . The reversible work W also equals the difference in entropy between the product streams "c" and "d", and the incoming stream "0", given by

$$W = -TS_{\text{out}} + TS_{\text{in}}$$

$$= 2 \cdot (V_c \cdot c_c \ln c_c + V_d \cdot c_d \ln c_d - V_0 \cdot c_0 \ln c_0), \tag{1}$$

where W and TS are expressed in units of  $k_BT$  when ion concentrations are in numbers per volume (multiply by RT when ion concentrations are expressed in mol/volume). The net work W must be a positive number because the reverse process of mixing two streams of unequal concentration is spontaneous.

We define  $\alpha$  as the ratio of dilute stream volume over the initial volume,  $\alpha=V_d/V_0$ . Using  $\alpha=(c_c-c_0)/(c_c-c_d)$ , Eq. (1) simplifies to

$$\frac{W}{V_d} = 2 \cdot \frac{c_0}{\alpha} \ln \frac{c_0 - \alpha \cdot c_d}{c_0 (1 - \alpha)} - 2 \cdot c_d \cdot \ln \frac{c_0 - \alpha \cdot c_d}{c_d (1 - \alpha)},\tag{2}$$

which expresses W per unit volume of dilute product  $V_d$  as function of the initial ion concentration  $c_0$ , the ion concentration of the dilute stream,  $c_d$ , and the volume ratio  $\alpha$ . Thus if the concentration of ions in the inflow  $c_0$  is known (namely the ionic strength, because we consider a 1:1 salt), as well as the separation factors  $\alpha$  and  $c_d$ , the reversible work is immediately calculated from Eq. (2). Fig. 2 gives calculation results for  $c_0 = 25$  mM as function of  $c_d$  and for various values of  $\alpha$ , where we have multiplied with RT to obtain W in J per unit volume. As expected, obtaining a certain dilute product volume  $V_d$ , of a certain concentration  $c_d$ , becomes energetically cheaper the lower the  $\alpha$ ; thus when more of the inflowing stream is discarded and the less it is concentrated. When  $\alpha$  goes to unity, thus the product stream "c" becomes infinitely concentrated, the required work goes to infinity.

Equation (2) can be compared with Eq. (B13) in Ref. [9] which is given by  $w^* = X_f \cdot X_b/(X_b - X_f) \cdot \ln(X_b/X_f)$ , where  $w^*$  is the work per unit dilute product volume  $V_d$ , and  $X_i$  is the "average mole fraction of total salts" in the feed "f" and the concentrated solution, brine, "b". The dilute product stream is assumed to be completely ion free. In that limit  $(c_d = 0)$ , Eq. (2) simplifies to  $W = -2 \cdot c_0 V_0 \ln(1 - \alpha)$ , and if we identify  $2 \cdot c_0$  with  $X_f$ ,  $2 \cdot c_c$  with  $X_b$ ,

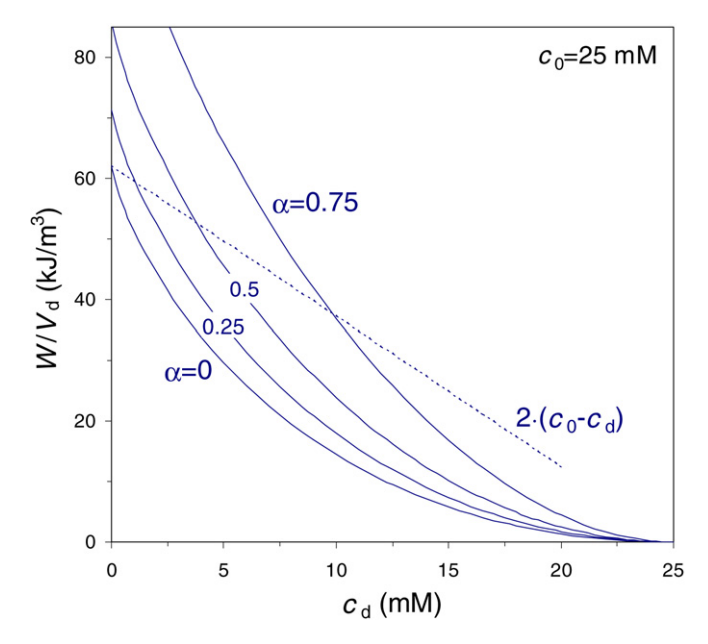


**Fig. 2.** Reversible work W per unit product volume to produce a dilute stream of ionic strength  $c_d$  from an ionic solution of ionic strength  $c_0 = 25$  mM, for various values of the volume ratio  $\alpha$ . The dashed line gives the "osmotic limit,"  $2 \cdot (\epsilon_0 - c_d)$ .

and  $\alpha$  with  $(X_b - X_f)/X_b$ , then the two equations do turn out to be exactly equal.

In the limit that  $\alpha$  is close to zero the dilute stream "d" is very small and the concentrated stream "c" has a concentration that is only marginally above that of the inflowing stream. In that case, Eq. (2) simplifies to

$$\frac{W}{V_d} = 2 \cdot (c_0 - c_d) - 2 \cdot c_d \ln \frac{c_0}{c_d}.$$
 (3)

Here, the first term might be identified as a kind of osmotic pressure difference between the inflowing and product stream. However, Eq. (3) shows that an additional, negative term is required which depends on the ratio of the two ion concentrations. Fig. 2 shows that the "osmotic term"  $2 \cdot (c_0 - c_d)$  (dashed line) gives the correct limit, either when *all ions* are to be removed  $(c_d = 0)$  or when *no ions* are removed  $(c_d = c_0)$ , but in between, i.e., for  $0 \le c_d \le c_0$ , the osmotic term significantly departs from the full result given by Eq. (3), even for small departures of  $c_d$  from zero or from  $c_0$ , with the required work much smaller than estimated from the osmotic term only. The maximum absolute departure of the osmotic term from the full result is found when  $c_d = c_0/e$ , which is around  $c_d \sim 9.2$  mM in the present calculation, where the deviation is  $2 \cdot RT \cdot c_d$ ; thus  $\sim 22.8$  kJ/m³. The maximum relative departure is found in the limit that  $c_d \rightarrow c_0$ .

## 3. Electrostatic double layer models

Next we will discuss the models for the polarization layers that will be used in the thermodynamic cycle analysis for charging and discharging. These models assume that the electrode is ideally polarizable; i.e., Faradaic electrochemical reactions are not considered. Also, chemical ion ad- or desorption at the inner or outer Helmholtz planes is not considered either. We use a Gouy–Chapman–Stern model for the double layers which we will supplement with a submodel for ion size constraints according to the Carnahan–Starling (CS) equation of state (as explained in more detail in Ref. [27] where further references to the theoretical liquid-state literature are provided). From this point onward we only consider a 1:1 monovalent salt solution. In both models, the total cell voltage  $V_{\rm cell}$  is divided over the two double layers, and is

a summation of the Stern layer voltage  $V_{\rm St}$  and the diffuse layer voltage  $V_d$ . Thus,

$$\frac{1}{2}V_{\text{cell}} = V_{\text{dl}} = V_{\text{St}} + V_d. \tag{4}$$

According to the Gouy-Chapman (Poisson-Boltzmann) model, the electric charge transferred is given by

$$\sigma = 4\frac{c_{\infty}}{\kappa} \cdot \sinh \frac{1}{2} \frac{V_d}{V_T},\tag{5}$$

where  $\sigma$  is a surface charge density in numbers per unit electrode area,  $\kappa$  is the inverse of the Debye length, given by  $\kappa^2=8\pi\lambda_Bc_\infty$ , where  $\lambda_B$  is the Bjerrum length ( $\lambda_B=0.72$  nm in water at room temperature),  $c_\infty$  is the ionic strength expressed in numbers per volume, and  $V_T=k_BT/e$  is the thermal voltage which is 25.6 mV at room temperature. Without a Stern layer,  $V_d=V_{\rm dl}$  and the relation  $\sigma-V_{\rm cell}$  is directly obtained from Eqs. (4) and (5).

When a Stern layer is included, Eq. (5) must be supplemented with Gauss' law at the Stern plane, given by

$$C_{St} \cdot V_{St} = \sigma \cdot e, \tag{6}$$

where e is the electron charge and  $C_{St}$  is the Stern layer capacity. The GCS model requires the simultaneous solution of Eqs. (4)–(6).

When we include volume effects using the CS model for ion volumetric interactions, no analytical solution is available. Instead we numerically solve the Poisson equation

$$\frac{d^2V}{dx^2} = -\frac{e}{\varepsilon_r \varepsilon_0} (c_+ - c_-),\tag{7}$$

where x is the place coordinate perpendicular to the interface, and  $c_+$  and  $c_-$  are the concentrations of cations and anions, respectively. Equation (7) is solved together with chemical equilibrium for both ion types,

$$\ln c_i + z_i \frac{e}{k_B T} V + \mu^{\text{ex}} = \ln c_\infty + \mu_\infty^{\text{ex}}, \tag{8}$$

where  $z_i$  is the charge sign (either +1 or -1), and  $\mu^{\rm ex}$  is given by the CS excess term

$$\mu^{\text{ex}} = \phi \frac{8 - 9\phi + 3\phi^2}{(1 - \phi)^3},\tag{9}$$

where  $\phi$  is the total local ion volume,  $\phi = v \cdot (c_+ + c_-)$  with v the ion volume, which is  $v = \pi/6 \cdot d_{\rm ion}^3$  with  $d_{\rm ion}$  the hydrated ion size.

Finally we require boundary conditions, which are V=0 far away from the interface, and  $V=V_d$  at the Stern plane, together with

$$\left. \frac{dV}{dx} \right|_{S_t} = -\frac{V_{St}}{d_{St}}.\tag{10}$$

In this Gouy–Chapman–Stern–Carnahan–Starling (GCS–CS) model, all of the above equations, Eqs. (4)–(10) are self-consistently solved to obtain the relation of  $\sigma$  vs  $V_{\rm cell}$ .

Fig. 3 shows calculation results for  $c_{\infty}=10$  mM for all three models which shows the well-known result that without a Stern layer the surface charge in the GC model exponentially increases with increasing voltage. This anomaly is due to the assumption of point charges that can reach the electrode infinitely close and there reach extremely high surface concentrations [28] (e.g., for a cell voltage of 1 V, and thus a voltage difference of 0.5 V over one diffuse layer, we have at the surface a counterion concentration which is increased by a factor of  $\exp(e/k_BT\cdot 0.5)\sim 10^9$ , which implies at room temperature and for  $c_{\infty}=10$  mM a surface concentration that is about  $10^5$  higher than that of the water molecules (55 M).

The GCS model is already much more realistic but still at 1 V cell potential and a Stern capacity of  $C_{\rm St}=2$  F/m<sup>2</sup> (and for  $c_{\infty}=10$  mM) we obtain unrealistically high ion concentrations at

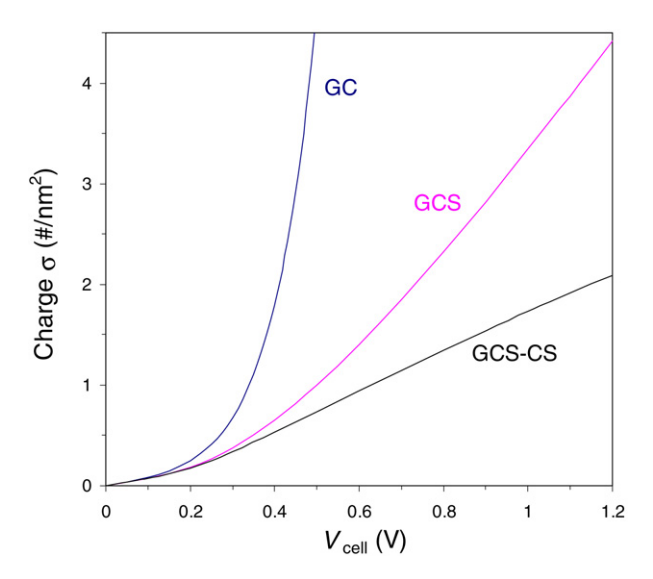


**Fig. 3.** Charge per unit electrode area as function of cell voltage for the GC, GCS, and GCS-CS models (explained in the text) at  $c_{\infty}=10$  mM,  $C_{\rm St}=2$  F/m², and a hydrated ion diameter of  $d_{\rm ion}=0.7$  nm.

the Stern plane, namely  $\sim$ 1.5 times the value of bulk water (which is 55 M). The resolution of this anomaly requires the inclusion of ion volume constraints in the diffuse part of the double layer. One option is to use the Stern–Bikerman–Freise model which includes ion volume constraints based on a lattice approach (Poisson–Fermi gas), which will limit the concentration at a chosen maximum packing density [29–31]. Here, however, we use a more exact, and off-lattice, expression for volume interactions in mixtures of hard spheres, namely by using the Carnahan–Starling equation of state. This implies that we implement in the ion chemical potential the  $\mu^{\rm ex}$  term given by Eq. (9). Now we obtain at the Stern plane concentrations that are much lower and more realistic; e.g., at a cell voltage of 1 V the ion concentration remains below 3.5 M.

# 4. Charge efficiency

In this section we will analyze the charge efficiency,  $\Lambda$ , which is the ratio between the amount of salt molecules removed from solution and the amount of electronic charge transferred between the electrodes. The charge efficiency  $\Lambda$  is always less than unity because the diffuse charge is partially due to counterion adsorption from solution, and partially due to co-ion expulsion from the polarization layers back into solution. Because of co-ion expulsion from the diffuse layers there is no 1:1 correspondence between the charge transferred and the amount of salt molecules removed. In the GC and GCS models it is possible to derive an analytical solution for  $\Lambda$  for an assumed planar structure of the polarization layer without overlap of opposite double layers. For a planar isolated diffuse layer, the Poisson–Boltzmann equation for the electric potential profile results in (assuming a 1:1 salt)

$$y(x) = 4 \cdot \operatorname{arctanh}\left(\exp(\kappa x) \cdot \tanh \frac{y_d}{4}\right),$$
 (11)

where  $y_d$  is the nondimensional electrical potential at the Stern plane relative to bulk solution (multiply y by the thermal voltage  $V_T$  to obtain the dimensional voltage V). The electronic charge that must be transferred from one electrode to the other is given by Eq. (5).

To calculate the salt adsorption  $\Gamma_{\rm salt}$  (and thus  $\Lambda$ ) we must take account of the fact that the counterion adsorption on one electrode "A" is partially negatively offset by the expulsion into solution of the same ion from the other electrode "B." The counterion adsorption on electrode A is given by an integration over the

diffuse layer volume of  $c_{\text{counterion}} - c_{\infty}$ , while the expulsion of the same ion (on the other electrode B) equals the expulsion of the coion from the diffuse layer at electrode A, given by an integration of  $c_{\infty} - c_{\text{co-ion}}$ . Now with  $c_{\text{counterion}} \cdot c_{\text{co-ion}} = c_{\infty}^2$ , the difference  $(c_{\text{counterion}} - c_{\infty}) - (c_{\infty} - c_{\text{co-ion}})$  simplifies to  $2 \cdot c_{\infty} \cdot (\cosh(y) - 1)$  which then needs to be integrated over the coordinate x to give the amount of salt removed per unit electrode area. Note that this analysis assumes that we deal with a symmetric salt solution and that we assume the two juxtaposed electrodes to be exactly the same (i.e., surface area and Stern capacity are the same).

Thus, the excess salt adsorption (amount of salt molecules removed from solution per unit electrode area),  $\Gamma_{\text{salt}}$ , can then be calculated as [32]

$$\Gamma_{\text{salt}} = 2c_{\infty} \int_{0}^{\infty} \{\cosh y - 1\} dx = \frac{8c_{\infty}}{\kappa} \sinh^{2} \frac{y_{d}}{4}.$$
 (12)

With the charge efficiency  $\Lambda$  being equal to the ratio  $\Gamma_{\rm salt}/\sigma$  we obtain from combining Eqs. (5) and (12) the simple relation

$$\Lambda = \tanh \frac{y_d}{4},\tag{13}$$

which interestingly predicts that  $\Lambda$  is independent of ionic strength. Rewriting Eq. (13) slightly, we can calculate that for a voltage difference between the two Stern planes of  $V^*$ , and with a thermal voltage of  $V_T \sim 25$  mV (room temperature),  $\Lambda$  is given roughly by  $\Lambda = \tanh(V^*/200$  mV). For example, for  $V^* = 200$  mV (corresponding to a total cell voltage of  $V_{\rm cell} = 240$  mV at  $c_\infty = 10$  mM and  $C_{\rm St} = 2$  F/m²), the removal efficiency is  $\Lambda = 76\%$ . At V = 400 mV it increases to 96% and at 600 mV it reaches 99.5%.

In Fig. 4a we show the removal efficiency for the GCS model for two values of the Stern capacity, namely  $C_{\text{St}} = 1$  and 2 F/m<sup>2</sup> as function of ionic strength. The ionic strength is of influence because of its effect—via Gauss' law at the Stern plane, Eqs. (5) and (6)—on the Stern layer voltage difference  $V_{\text{St}}$ . Certainly at higher ionic strength and lower Stern capacity,  $\Lambda$  deviates significantly from unity.

In Fig. 4b we compare for  $C_{St} = 2 \text{ F/m}^2$  predictions of the GCS model with those of the GCS-CS model, which includes ion volume constraints in the diffuse part of the polarization layer. At  $c_{\infty} = 10$  mM the predictions are similar in both models, though there are still significant differences: e.g., at  $V_{\text{cell}} = 1 \text{ V}$ ,  $\Lambda$  remains 5% away from 100% in the GCS-CS model, but only 2% in the GCS model. For  $c_{\infty}=100$  mM the additional deviation from  $\Lambda=100\%$ when volume effects in the diffuse layer are included (namely in the GCS-CS model) is even more significant, with at  $V_{\text{cell}} = 1 \text{ V}$ ,  $\Lambda = 83\%$  in the GCS-CS model, while it is  $\Lambda = 94\%$  in the GCS model. For 1 mM salt the situation is rather different and unexpected, with first of all an almost exact fit between the two models up to a cell voltage of  $\sim 0.5$  V. However, beyond  $V_{\text{cell}} = 0.5$  V a very significant difference develops: whereas the charge efficiency  $\Lambda$  steadily increases with increasing  $\Lambda$  in the GCS-model, in the GCS-CS model the charge efficiency  $\Lambda$  goes down again beyond  $V_{\rm cell} = 0.5$  V, and significantly so, to reach a value of  $\Lambda = 88\%$  at  $V_{\rm cell}=1$  V, whereas at this point the charge efficiency is  $\Lambda=99\%$ in the GCS model. At higher voltage  $\Lambda$  in the GCS-CS model increases again.

## 5. Thermodynamic cycle analysis

Based on the relation between charge  $\sigma$  vs cell voltage  $V_{\rm cell}$  it is possible to analyze the work that is exerted on the system W for a single charging (ion removal) step, if the bulk solution concentration is constant. Namely this is given by the integral  $\int_0^{\sigma_{\rm final}} V_{\rm cell} \, d\sigma$  times the electron charge e to give the reversible energy required for charging 1 nm² of electrode surface in a constant

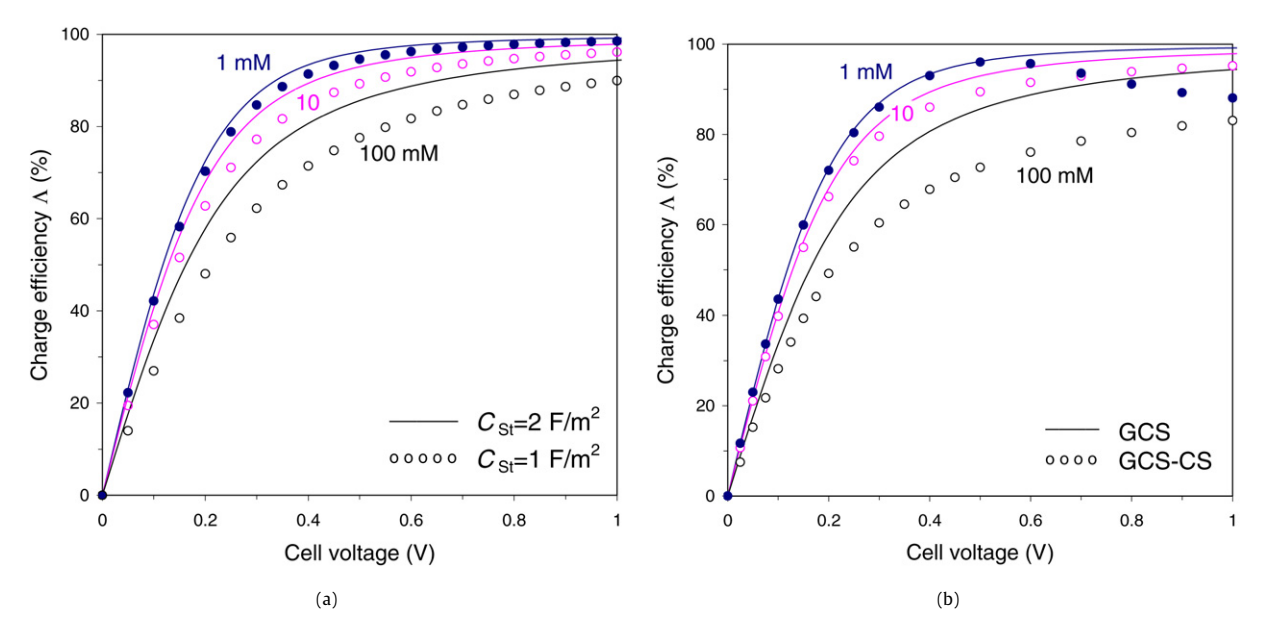


**Fig. 4.** The charge efficiency Λ: the number of salt molecules removed from solution per electron transferred as function of cell voltage, Stern capacity, and ionic strength. (a) According to the GCS model. Only at a high Stern capacity, low ionic strength, and high cell voltage is the removal efficiency Λ close to unity. (b) According to the GCS and GCS-CS models (ion size 0.7 nm,  $C_{St} = 2 \text{ F/m}^2$ ).

ionic strength solution (see Eq. (7b) in Ref. [6]). In Fig. 3, this integral is represented by the area above one of the curves, bounded by a horizontal line which describes  $\sigma_{\rm final}$ . Interestingly, the more that volume constraints are considered the *higher* is W to reach the same value of  $\sigma_{\rm final}$ . However, when charging continues until a certain value of  $V_{\rm cell}$  is reached, then the situation is exactly reversed: going from the GC model to the GCS model the required work is *lower*, and W is even lower for the GCS-CS model.

Now, when charging is no longer reversible (which can be achieved by very slowly increasing the applied voltage), but occurs irreversibly, namely by directly applying the final required voltage  $V_{\rm cell,final}$ , the work input is given by the product of  $\sigma_{\rm final} \cdot V_{\rm cell,final}$ . For the GCS model and for charging up to  $\sigma_{\rm final} = 2~\#/{\rm nm}^2$ , the required work input for the irreversible process is an additional  $\sim 55\%$  higher than for the reversible process. For the GC model the difference between reversible and irreversible is smaller, namely an additional  $\sim 30\%$ , but for the most realistic GCS-CS model, the difference between reversible and irreversible charging is  $\sim 83\%$ ; i.e., when we directly apply  $V_{\rm cell,final} = 1.15~V$  (which leads to  $\sigma_{\rm final} = 2~\#/{\rm nm}^2$ ) the work input will be 83% higher than when we would gradually and slowly increase  $V_{\rm cell}$  from zero to  $V_{\rm cell,final}$ .

Next we will analyze a charging-plus-discharging cycle and find out that this difference between reversible (minimum) work and irreversible work increases further. First of all we must realize that the thermodynamic work as derived from Fig. 3 assumes a constant background ionic strength during deionization. However, in reality we will gradually go from the initial to the final concentration during the process (during charging from  $c_0$  to  $c_d$ , and during discharging from  $c_d$ —via  $c_0$ —to  $c_c$ ). To analyze these effects we envision a batchwise operation in which we first add the solution volume that needs to be depleted from ions  $(V_d)$ . When the desired removal efficiency has been achieved (the ion concentration has been reduced from  $c_0$  to  $c_d$ ), this volume is removed from the cell and fresh solution of volume  $V_c$  is added, into which the ions adsorbed on the electrodes will gradually dissolve to generate the concentrate of concentration  $c_c$ . Thus, the work calculated on the basis of Fig. 3 is not the work input during charging, but instead a trace is followed of points  $\sigma$  vs  $V_{\text{cell}}$  while the ionic strength gradually varies from  $c_0$  to  $c_d$  (see Fig. 5).

How do we calculate the exact trace that the process follows during the charging-discharging process? Let us assume that we start with a solution at  $c_0 = 20$  mM, which we aim to split in a volume at  $c_d = 10$  mM and a volume at  $c_c = 40$  mM (see Fig. 5a) ( $\alpha = 2/3$ ). To make a calculation we assume that we run the process in a batch mode. First 2/3 liter of 20 mM solution is brought in the cell which is charged such that the solution concentration is reduced to 10 mM. Then this solution is removed from the cell and 1/3 liter still at 20 mM is fed to the cell. In the discharge step the ion concentration in this volume will increase to 40 mM. Important is the realization that during the replacement of dilute solution by fresh solution the salt adsorption must remain constant. This means that in this replacement, or "switching," step a trace is followed which is not horizontal (which would be constant charge  $\sigma$ ) or vertical (constant  $V_{\rm cell}$ ), but instead is curved as shown in Fig. 5 (upper right part of each cycle).

The enclosed area of the trace ("cycle") is the net work that has gone into the system and which has been transferred into a decrease of entropy of the two product streams. This is work which is not recoverable, and which has inevitably gone into the making of the product streams (i.e., the entropy of the ionic solution that passed through the cell has decreased). On the microscale we can say this net work input is due to the fact that on discharging the ionic strength in the cell is higher than on charging, and that the charge vs  $V_{\rm cell}$  curve is shifted upward at higher ionic strength. From our macroscopic thermodynamic analysis we already knew a priori that inevitably somewhere a difference had to develop between the work input during charging and the work recovery on discharging.

Let us continue the detailed calculation. We will use a cell voltage of 1 V and assume a Stern capacity of  $C_{\rm St}=2~{\rm F/m^2}$ . We make a calculation based on the GCS model (because the GCS-CS model is very complicated to solve for a full cycle). First we solve the GCS model to find that for the required ionic strength of the dilute flow  $c_d=10~{\rm mM}$  and the given cell voltage of 1 V the required electrode area is 1227 m² (for each electrode) and the surface charge at the end of the charging step will be  $\sigma_{\rm I}=3.34~{\rm mm^{-2}}$ . The trace is calculated from the GCS model supplemented with a salt balance given by

$$\sigma \cdot \frac{1}{N_{\text{av}}} \cdot \Lambda \cdot A = V_d \cdot (c_0 - c), \tag{14}$$

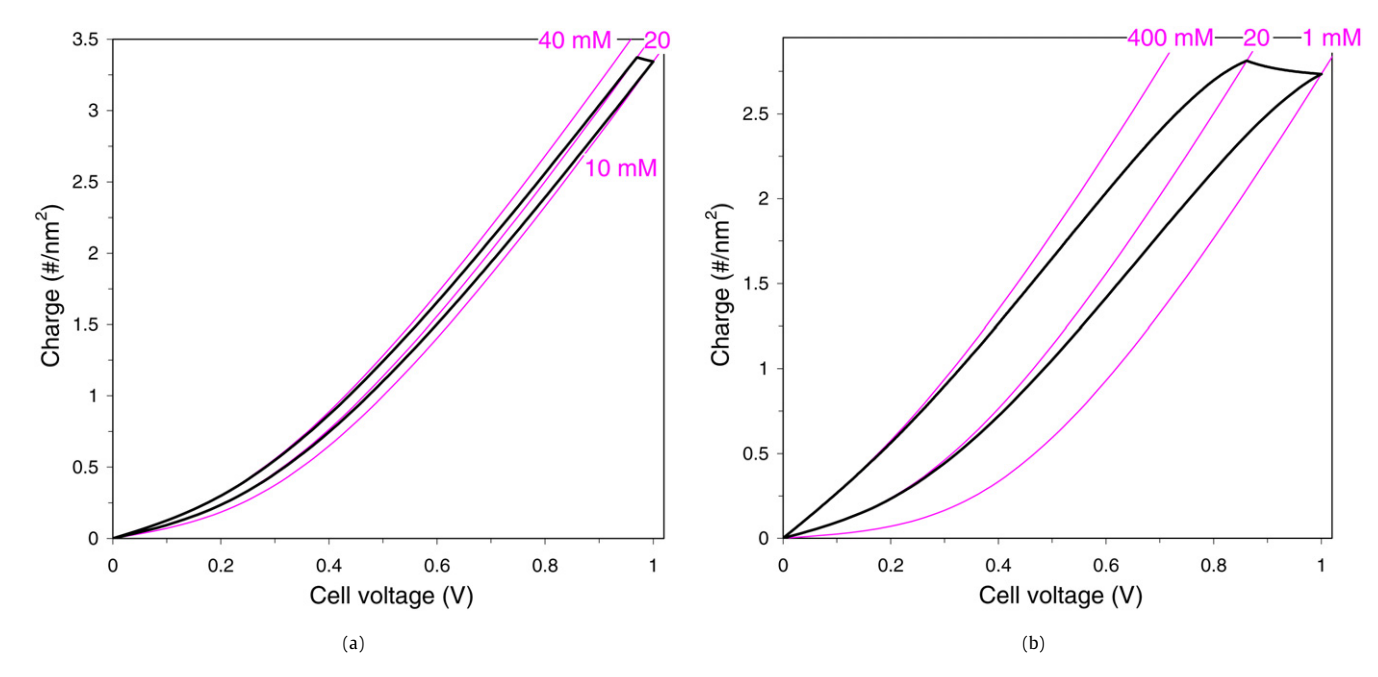


Fig. 5. Charge density as function of voltage for the GCS model at different ionic strengths (thin lines,  $C_{St} = 2 \text{ F/m}^2$ ). In bold the  $V - \sigma$  trajectory (thermodynamic cycle) during an idealized batch deionization experiment. The enclosed area is the net work that must be performed in a purely reversible process.

where c is the bulk salt concentration which slowly decreases from  $c_0$  to  $c_d$  during the charging step, and which determines the timedependent value for the Debye length  $1/\kappa$ , and in this way influences the charge-voltage relation of Eq. (5). From the analysis, the reversible work on charging is calculated to be  $W_I = 402.44 \text{ J}$  (obtained from  $\int_0^{\sigma_1} V_{\text{cell}} d\sigma$  according to the charging trace in Fig. 5a, and multiplied with the electron charge e and electrode area A). The several phases of the thermodynamic cycle based on the balances (14)-(16) can only be analyzed numerically as during the gradual change of the salt concentration c, both the charge  $\sigma$ and the charge efficiency  $\Lambda$  change, which are coupled through the GCS model, Eqs. (4)-(6) and (13), while the reversible energy then follows from a numerical integration of  $V_{\text{cell}}$  over  $\sigma$ . Note that concentrations c in Eqs. (1)–(3) and (14)–(16) denote the ionic strength of the solution in the CDI cell, which is denoted by  $c_{\infty}$  in Eqs. (5), (8), and (12).

Next we analyze the salt replacement "switching" step (upper right part of the trace in Fig. 5), following the same procedure but with the salt balance as closure equation,

$$\Gamma_{\text{salt}} = \sigma \cdot \Lambda,$$
 (15)

where  $\Gamma_{\rm salt}$  is constant (3.272 nm<sup>-2</sup>). In this step the additional work is  $W_{\rm II}=5.69$  J, and we arrive after this step at  $V_{\rm cell,II}=0.97$  V and  $\sigma_{\rm II}=3.373$  nm<sup>-2</sup>. Finally we analyze the discharge step based on the balance

$$\sigma \cdot \frac{1}{N_{\text{av}}} \cdot \Lambda \cdot A = V_c \cdot (c_c - c), \tag{16}$$

resulting in  $W_{\rm III} = -385.23$  J. The difference  $W_{\rm I} + W_{\rm II} - W_{\rm III}$  is given by  $W_{\rm rev} = 22.90$  J. This result can be compared with the thermodynamic calculation based on Eq. (2). As hoped for, exactly the same result is obtained.

The advantage of the cycle analysis (which is much more complicated than the thermodynamic calculation) is that we can analyze the energy efficiency of a process that is not run fully reversible, compared to the fully reversible case. For instance, in a standard experiment we apply right from the start the final voltage, which requires for the charging (ion removal) step a work input of  $W_{\rm irr,ch} = 657.42$  J. Assuming a reversible switching step (phase II) which costs W = 5.69 J and assuming no

useful work output during discharge (e.g., because the electric circuit is short-circuited, or the electric current simply runs through a resistance producing heat), the total irreversible work input is  $W_{\rm irr}=663.11$  J, and the energy efficiency can be calculated as  $\eta=3.5\%$ . Thus this analysis suggests that the irreversible process in the way it is typically operated in the laboratory can be improved in energy efficiency by a factor of almost 30 in this case.

In Fig. 5b we show results for a more extreme separation, namely a separation of the 20 mM starting solution into a dilute stream of 1 mM and a concentrate stream of 400 mM ( $\alpha \sim 0.95$ ). Here the total reversible work is  $W_{\rm rev} = 269$  J, almost 12 times as expensive as a separation in  $c_d = 10$  and  $c_c = 40$  mM. However, if we run this process in the irreversible fashion as discussed above, the energy cost would be  $W_{\rm irr} = 1807$  J, which is "only"  $\sim 7$  times higher than the energy requirement of the reversible process ( $\eta = 15\%$ ). Thus, the more extreme the separation, the smaller the difference between reversible and irreversible operation, and the closer we are already to ideal operation ( $\eta = 1$ ) when we directly apply the maximum voltage and do not recover work during discharging.

The above calculation was based on the assumption that we discharge the cell fully, down to a charge and cell voltage of zero. However, in reality this is much too time-consuming and instead we would already like to switch back from discharging to charging when the electrodes are not yet completely discharged. This situation is analyzed in Fig. 6 where the final cell voltage is 1 V in all cases, but we start the charging cycle not at 0 V, but at 0.3 and 0.65 V (black and red curves, respectively). With increasing initial voltage we see that the enclosed area representing the reversible work input decreases, which is exactly compensated by the fact that we need proportionally more electrode surface area ( $A \sim 4000 \text{ m}^2$  at a starting voltage of 0 V,  $\sim 4600 \text{ m}^2$  at 0.30 V, and 10,600 m<sup>2</sup> at 0.65 V), because the total minimal, reversible work must obviously be independent of the details of how the separation process is operated. However, the differences in energy efficiency are large between processes operating at different initial voltages. If we analyze the irreversible process as discussed above (directly apply 1 V, reversible switching step, and no energy recovery during discharge) the efficiency  $\eta$  goes down from  $\eta = 15\%$ when the minimum voltage is 0 V (as in Fig. 5b), to  $\eta = 13\%$  at

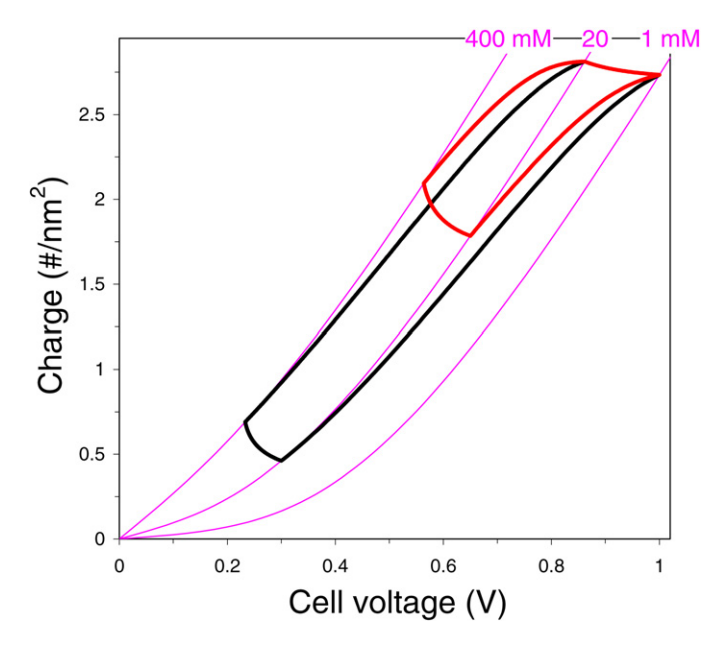


**Fig. 6.** Thermodynamic cycle for capacitive deionization. Same as Fig. 5b but with the charging step starting at a nonzero voltage.

0.3 V and to only  $\eta=5.6\%$  at 0.65 V. Clearly the higher the minimum voltage the more important is a close-to-reversible design of the CDI technology.

The present calculation scheme is based on ideal batchwise operation of the CDI unit. In reality, however, operation goes in a constant throughflow mode in which the ionic solution continuously enters and leaves the unit, with the effluent ion concentration continuously changing in time. The thermodynamic and process analysis of CDI in such a throughflow model is much more complicated than for the present calculation scheme based on ideal sequential batchwise operation, and will be taken up in future work, extending on the theory as presented in the present work.

#### 6. Conclusions

For noninteracting pointlike ions (ideal gas behavior), expressions were derived for the reversible thermodynamic work required to separate an ionic solution into a more dilute and a more concentrated flow. The required work is fully utilized to decrease the entropy of the system and increases with increasing the amount of dilute volume to be produced from the starting solution. Several electrostatic double layer models are analyzed to describe ion removal using capacitive deionization (CDI). To keep the ion concentration at the Stern plane at realistic values of several M, ion volume constraints in the diffuse part of the double layer must be implemented, besides the Stern layer capacity. Analysis of a

full charging–discharging thermodynamic cycle using the Gouy–Chapman–Stern model and assuming an ideal batchwise operation of CDI gives exactly the same reversible work as a macroscopic thermodynamic calculation. The charge efficiency,  $\Lambda$ , which is the number of salt molecules removed for each electron transferred from one electrode to the other, only approaches unity for high cell voltage, a high Stern layer capacity, and a low ionic strength. Unexpectedly, in the most realistic model, which also includes ion volume effects in the diffuse part of the polarization layer,  $\Lambda$  does not monotonically increase with cell voltage, but reaches a maximum value after which it again significantly decreases.

## Acknowledgments

I thank B. van der Wal (Voltea B.V.) for useful discussions during preparation of this manuscript. Voltea B.V. (Leiden) is kindly acknowledged for financial support.

## References

- [1] B.B. Arnold, G.W. Murphy, J. Phys. Chem. 65 (1961) 135.
- [2] G.W. Murphy, D.D. Caudle, Electrochim. Acta 12 (1967) 1655.
- [3] A.M. Johnson, J. Newman, J. Electrochem. Soc. 118 (1971) 510.
- [4] A. Soffer, M. Folman, Electroanal. Chem. 38 (1972) 25.
- [5] Y. Oren, A. Soffer, J. Electrochem. Soc. 125 (1978) 869.
- [6] Y. Oren, A. Soffer, J. Appl. Electrochem. 13 (1983) 473.
- [7] J.C. Farmer, D.V. Fix, G.V. Mack, R.W. Pekala, J.F. Poco, J. Appl. Electrochem. 26 (1996) 1007.
- [8] M.D. Andelman, Filtr. Separat. 35 (1998) 345.
- [9] K.S. Spiegler, Y.M. El-Sayed, Desalination 134 (2001) 109.
- [10] T.J. Welgemoed, C.F. Schutte, Desalination 183 (2005) 327.
- [11] H.-J. Oh, J.-H. Lee, H.-J. Ahn, Y. Jeong, Y.-J. Kim, C.-S. Chi, Thin Solid Films 515 (2005) 220.
- [12] J.-B. Lee, K.-K. Park, H.-M. Eum, C.-W. Lee, Desalination 196 (2006) 125.
- [13] D. Oi, L. Zou, E. Hu, Res. J. Chem. Environ. 11 (2007) 92.
- [14] P. Xu, J.E. Drewes, D. Heil, G. Wang, Water Res. 42 (2008) 2605.
- [15] L. Zou, G. Morris, D. Qi, Desalination 225 (2008) 329.
- [16] L. Zou, L. Li, H. Song, G. Morris, Water Res. (2008), in press.
- [17] B.E. Conway, Electrochemical Supercapacitors, Kluwer, New York, 1999.
- [18] J.P. Zheng, T.R. Jow, J. Electrochem. Soc. 144 (1997) 2417.
- [19] G. Salitra, A. Soffer, L. Eliad, Y. Cohen, D. Aurbach, J. Electrochem. Soc. 147 (2000) 2486.
- [20] A. Burke, J. Power Sour. 91 (2000) 37.
- [21] R. Kötz, M. Carlen, Electrochim. Acta 45 (2000) 2483.
- [22] A.K. Shukla, S. Sampath, K. Vijayamohanan, Curr. Sci. 79 (2000) 1656.
- [23] K.-L. Yang, T.-Y. Ying, S. Yiacoumi, C. Tsouris, E.S. Vittoratos, Langmuir 17 (2001) 1961.
- [24] Y.M. Vol'fkovich, T.M. Serdyuk, Russ. J. Electrochem. 38 (2002) 935.
- [25] B. Kastening, M. Heins, Electrochim. Acta 50 (2005) 2487.
- [26] M.D. Stoller, S. Park, Y. Zhu, J. An, R.S. Ruoff, Nano Lett. (2008), in press.
- [27] P.M. Biesheuvel, M. van Soestbergen, J. Colloid Interface Sci. 316 (2007) 490.
- [28] D.C. Grahame, Chem. Rev. 41 (1947) 441.
- [29] O. Stern, Z. Elektrochem. 30 (1924) 508.
- [30] J.J. Bikerman, Philos. Mag. 33 (1942) 384.
- [31] Z. Freise, Z. Elektrochem. 56 (1952) 822.
- [32] M.Z. Bazant, K. Thornton, A. Ajdari, Phys. Rev. E 70 (2004) 021506.